American Mineralogist, Volume 97, pages 1676–1684, 2012

The temperature and compositional dependence of disordering in Fe-bearing dolomites

Ettore Franzolin,[1] Marco Merlini,[2] Stefano Poli,[2,*] and Max W. Schmidt[1]

[1]Institute of Geochemistry and Petrology, ETH Zurich, 8092 Zurich, Switzerland
[2]Dipartimento di Scienze della Terra, Università degli Studi di Milano, 20133 Milano, Italy

Abstract

Dolomite occurs in a wide range of rock compositions, from peridotites to mafic eclogites and metasediments, up to mantle depths of more than 200 km. At low-temperatures dolomite is ordered ($R\bar{3}$), but transforms with increasing temperature into a disordered higher symmetry structure ($R\bar{3}c$).

To understand the thermodynamics of dolomite, we have investigated temperature, pressure, kinetics, and compositional dependence of the disordering process in Fe-bearing dolomites. To avoid quench effects, in situ X-ray powder diffraction experiments were performed at 300–1350 K and 2.6–4.2 GPa. The long-range order parameter *s*, quantifying the degree of ordering, has been determined using structural parameters from Rietveld refinement and the normalized peak area variation of superstructure Bragg peaks characterizing structural ordering/disordering. Time-series experiments show that disordering occurs in 20–30 min at 858 K and in a few minutes at temperatures ≥999 K. The order parameter decreases with increasing temperature and X_{Fe}. Complete disorder is attained in dolomite at ~1240 K, 100–220 K lower than previously thought, and in an ankeritic-dolomite$_{s.s.}$ with an X_{Fe} of 0.43 at temperatures as low as ~900 K. The temperature-composition dependence of the disorder process was fitted with a phenomenological approach intermediate between the Landau theory and the Bragg-Williams model and predicts complete disorder in pure ankerite to occur already at ~470 K.

The relatively low-temperature experiments of this study also constrain the breakdown of dolomite to aragonite+Fe-bearing magnesite at 4.2 GPa to temperature lower than ~800 K favoring an almost straight Clapeyron-slope for this disputed reaction.

Keywords: Carbonates, high pressure, synchrotron, dolomite

Introduction

Natural evidence, experimental studies, and phase equilibria calculations demonstrate that carbonates are stable in the mantle and in most crustal bulk compositions for a wide range of *P*, *T*, and f_{O_2}. Even though the composition of carbonates in CO_2-bearing systems is very dependent on temperature, pressure, and bulk composition, carbonates with dolomitic composition are generally stable at pressure up to 2.7–3 GPa in peridotites (Wallace and Green 1988; Falloon and Green 1989; Dasgupta and Hirschmann 2006; Tumiati et al. 2012), to 2–7 GPa in mafic eclogites (Molina and Poli 2000; Hammouda 2003; Yaxley and Brey 2004; Dasgupta et al. 2004, 2005; Poli et al. 2009) and to 8 GPa in carbonated metapelites (Grassi and Schmidt 2011). Nevertheless, dolomite is not the only stable carbonate at pressures lower than 6 GPa; the pair dolomite+magnesite, for example, has been synthesized by Molina and Poli (2000), Dasgupta et al. (2004), and Poli et al. (2009) up to 4.5 GPa in carbonate bearing mafic eclogites.

The pressure stability of dolomite to high pressure is confined by the reaction dolomite = magnesite+aragonite. In a compositional space approaching the pure system CaO-MgO-CO_2, this reaction occurs at >5 GPa at temperatures ≥1100–1200 K but the different studies yielded large discrepancies in the position and the dP/dT slope of the reaction at <5 GPa: the studies of Martinez et al. (1996), Sato and Katsura (2001), and Morlidge et al. (2006) found a straight Clapeyron slope of ~7.5 MPa/K for this reaction, while others have a slightly steeper slope of 12 MPa/K at >1200 K and a sharp bent to a *P*-*T* slope of <2 MPa/K at <1000 K (Luth 2001; Shirasaka et al. 2002; Buob et al. 2006). Hammouda et al. (2011) found a similar high-temperature slope, but a moderate bent to a slope of ~3.3 MPa/K at <1000 K. Whether or not the proposed change in slope near 5 GPa (Luth 2001; Buob et al. 2006) and the exact *P*-*T* position of this reaction might be ascribed to dolomite impurities and/or ordering phenomena has still to be largely explored.

Complex solid solution relations between disordered "calcite like" structures ($R\bar{3}c$) and ordered "dolomite like" structures ($R\bar{3}$) characterize the carbonates. The structure of the ordered compound (i.e., dolomite) is made of alternating layers of Ca^{2+} and Mg^{2+} in octahedral coordination, intercalated by planar CO_3^{2-} groups, defining M1 and M2 sites, which can preferentially host Ca or Mg, respectively. With increasing temperature Ca and Mg exchange between the two octahedral sites up to the critical temperature, where M1 and M2 become undistinguishable and the disordered higher symmetry structure $R\bar{3}c$ becomes stable. The degree of ordering can be quantified with the long-range order (LRO) parameter $s = 2X_{Ca}^{M1} - 1$, where X_{Ca}^{M1} is the mole fraction of Ca hosted in the M1 site. The long-range order parameter *s* varies between 1 at low temperature, when the structure is perfectly ordered, and 0 above the critical temperature (T_c), when the structure is completely disordered.

* E-mail: stefano.poli@unimi.it

0003-004X/12/0010–1676$05.00/DOI: http://dx.doi.org/10.2138/am.2012.4126

To overcome reordering phenomena induced by quench, Antao et al. (2004) employed synchrotron in situ X-ray diffraction to investigate the state of order in dolomite as a function of temperature. They observed the occurrence of the $R\bar{3} \leftrightarrow R\bar{3}c$ phase transition at 1466 K and 3.0 GPa. More recently Hammouda et al. (2011) investigated with in situ techniques the disordering of dolomite between 3.37 and 4.05 GPa observing the occurrence of the fully disordered structure at 1340 K. The existing studies on order-disorder are limited to almost pure Mg-dolomite, thus the role of Fe on ordering in the dolomite-ankerite solid solution remains completely unconstrained but is crucial to understand the thermodynamics and phase relations in the ternary $CaCO_3$-$MgCO_3$-$FeCO_3$ system.

Miscibility gaps and phase relations have been extensively studied by Goldsmith et al. (1962), Rosenberg (1967), and Franzolin et al. (2011) in the system $CaCO_3$-$MgCO_3$-$FeCO_3$, who proposed a solid-solution model for ternary carbonates valid up to 6 GPa. Because disordering phenomena were undetermined for compositions other than Fe-poor dolomite, the aim of this study is to investigate structural changes associated with order-disorder reactions in the ternary $CaCO_3$-$MgCO_3$-$FeCO_3$ system. Experiments have been performed at high *P-T* conditions (2.6 to 4.2 GPa, 300–1350 K) coupling a Paris-Edinburgh apparatus with in situ X-ray powder diffraction.

In this study, we use X_{Fe} or X_{Mg} as the atomic fraction of Fe or Mg over Fe+Mg and the term X_{Ca} for Ca/(Ca+Mg+Fe). The term Mg-calcite is employed for any carbonate that is Ca-enriched with respect to the join dolomite-ankerite, i.e., $X_{Ca} > 0.6$.

Experimental methods

Sample selection and preparation

Samples Dol1 and Dol2 (Table 1) are natural Fe-bearing dolomite from Adamello, with a chemical composition close to $Ca_{0.49}Mg_{0.47}Fe_{0.04}(CO_3)$ (Gieré 1990). This specimen is intermediate between the Fe-poor dolomites investigated by Hammouda et al. (2011) [Nyaoulou dolomite, $Ca_{0.465}Mg_{0.465}Fe_{0.07}(CO_3)$], Luth (2001) and Antao et al. (2004) [Eugui dolomite, $Ca_{0.501}Mg_{0.494}Fe_{0.005}(CO_3)$], and the almost pure dolomite of Shirasaka et al. (2002) [Burumodo dolomite, $Ca_{0.494}Mg_{0.504}Fe_{0.001}Mn_{0.001}(CO_3)$]. The samples S2, S4, S5, and S6 are synthetic and were chemically and texturally equilibrated in piston-cylinders at ETH Zurich, employing assemblies made of teflon-NaCl-pyrex-graphite-MgO. The starting materials for these synthesis were mixed from almost pure natural magnesite from Obersdorf (Philipp 1998) and from synthetic calcite and siderite. The latter has been synthesized in externally heated cold seal vessels at 200 MPa and 350 °C from iron oxalate sealed into gold capsules following French (1971). To avoid major siderite oxidation, synthesis experiments have been run with inner graphite capsules placed in a welded Pt capsule. Temperature was controlled within ±2 °C, using B-type ($Pt_{94}Rh_6/Pt_{70}Rh_{30}$) thermocouples. The Fe-bearing dolomites have been synthesized at 2 GPa and 973 K for 168 h. Afterward, S4 and S6 have been re-equilibrated at 400 °C for 48 h, while S2 has been re-equilibrated at 573 K.

Table 1. Composition of the samples used in this study

Sample	Composition	Fe/(Fe+Mg) (X_{Fe})	Ca/(Ca+Mg+Fe)
Dol1	$Ca_{0.49}Mg_{0.47}Fe_{0.04}CO_3$	0.08	0.49
Dol2	$Ca_{0.49}Mg_{0.47}Fe_{0.04}CO_3$	0.08	0.49
S2	$Ca_{0.54}Mg_{0.26}Fe_{0.20}CO_3$	0.43	0.54
S4	$Ca_{0.52}Mg_{0.40}Fe_{0.08}CO_3$	0.17	0.52
S5	$Ca_{0.83}Mg_{0.12}Fe_{0.05}CO_3$	0.29	0.83
S6	$Ca_{0.51}Mg_{0.46}Fe_{0.03}CO_3$	0.06	0.51
Eugui	$Ca_{0.501}Mg_{0.494}Fe_{0.005}CO_3$	0.01	0.50
Nyaoulou	$Ca_{0.465}Mg_{0.465}Fe_{0.07}CO_3$	0.13	0.465
Burumodo	$Ca_{0.494}Mg_{0.504}Fe_{0.001}Mn_{0.001}(CO_3)$	0.001	0.494

Note: Composition of the Eugui dolomite used by Antao et al. (2004) and Luth (2001), Nyaoulou dolomite by Hammouda et al. (2011), and Burumodo dolomite by Shirasaka et al. (2002) are reported for comparison.

To synthesize highly ordered samples, a slow cooling rate of 1 °C/min has been employed. The synthesis S5 has been run at 1373 K for 72 h and fast quenched. It is important to point out that minor quantities of magnetite, a product of siderite oxidation, have been detected by powder XRD in all synthesis products. Magnetite was therefore detected, as a relict, in most in situ collection as a trace phase. A small fraction of each synthesized sample was embedded in epoxy and analyzed by electron microprobe (JEOL JXA8200) at ETH to determine the final chemical composition (Table 1; for analytical details see Franzolin et al. 2010).

Synchrotron X-ray powder diffraction

In situ, synchrotron X-ray powder diffraction (XRPD) experiments were performed at the high pressure and temperature beamline ID27 at the European Synchrotron Radiation Facility (Grenoble, France). The standard experimental setup of ID27 has been used, employing a monochromatic beam [$\lambda = 0.37380(1)$ Å], the Paris-Edinburgh large volume press (Besson et al. 1992), Soller slits to shield the diffraction signal from the gasket, and an area detector (image plate, MAR 345 system). The starting material has been put directly inside the graphite furnace, which constrains oxygen fugacity to CCO as an upper bound. Pressure was first increased to approximately the desired value and then temperature increased in defined time steps from room temperature to the critical temperature and back to room temperature. MgO and Au, placed both at the same end of the sample to prevent reaction therewith, have been used as *P-T* calibrants, following a procedure described by Crichton and Mezouar (2002) and Antao et al. (2004).

A water-cooling system mounted on the tungsten carbide anvils was used to reduce variations of pressure upon heating to <2% at the maximum temperature (Mezouar et al. 1999). The pressure variations, which amount to <0.2 GPa at the *P-T* conditions investigated here, propagate to temperature variations calculated from the EoS of MgO and Au of <30 K. The overall accuracy of temperature is thus estimated to ~50 K. An indirect confirmation of such an accuracy may be derived from the calculated thermal expansion of dolomite at 3 GPa. Using the formalism after Holland and Powell (1998), $V = V_0[1 + a^0(T - T_0) + 20a^0(\sqrt{T} - \sqrt{T_0})]$, we extracted the thermal expansion coefficient for dolomite [$a^0 = 61(3)\cdot10^{-6}$ K^{-1}]. This value matches the trend between calcite [$a^0 = 47(2)\cdot10^{-6}$ K^{-1}] and magnesite [$a^0 = 67(3)\cdot10^{-6}$ K^{-1}], whose thermal expansion coefficients have been extracted with the same approach using data reported by Markgraf and Reeder (1985). As the pressure dependence of thermal expansion in carbonates is small over the pressure range 0–3 GPa (Wu et al. 1995), the value obtained in this study testifies for accurate experimental temperatures.

Synchrotron XRPD at ambient conditions have also been collected from carbonates synthesized in piston cylinders at 3.5 GPa (Appendix Table 1[1]) on ID09 beamline [$\lambda = 0.41453(1)$ Å, Mar555 area detector]. These powder diffractogramms were employed to determine to what extent disordering is quenchable in conventional quench-experiments. The results on quenchability are necessary to be able to compare quench with in situ experiments.

Analytical strategy

The two-dimensional area detector XRPD images reveal a very limited recrystallization of the starting material on heating at high pressure (Fig. 1) when synthetic samples were used (S2, S4, S6). On the contrary, the experiments performed with natural dolomite, reveal a textured powder pattern. For this reason, only the samples S2, S4, and S6 allow a reliable structural refinement on the integrated powder pattern (Fit2D software, Hammersley et al. 1996). The results of Rietveld refinement on dolomite sample suffered some systematic errors, detectable for example from interatomic distances even when including a "preferred orientation" correction. A better statistics in experiments S2, S4, and S6 can be explained by the very small size of crystallites in synthetic starting material.

We therefore decided to perform Rietveld refinement, to extract accurate lattice parameters for all the samples, but use refined structural data only for the samples presenting continuous diffraction rings.

Disordering kinetics

To test the dolomite disordering kinetics, XRPD spectra have been collected as a function of time at isothermal conditions for sample Dol1 at 3.4 GPa (Ap-

[1] Deposit item AM-12-075, Appendix Tables and Figure. Deposit items are available two ways: For a paper copy contact the Business Office of the Mineralogical Society of America (see inside front cover of recent issue) for price information. For an electronic copy visit the MSA web site at http://www.minsocam.org, go to the *American Mineralogist* Contents, find the table of contents for the specific volume/issue wanted, and then click on the deposit link there.

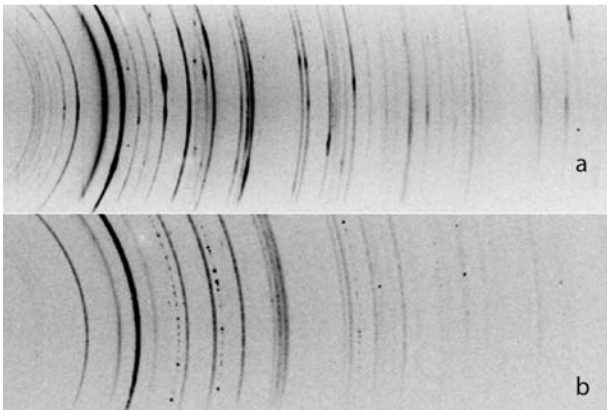

FIGURE 1. Synchrotron powder X-ray diffraction image for synthetic samples (**a**) dolomite (Dol1) at 3.2 GPa 1089 K, (**b**) S4 at 2.8 GPa 1047 K revealing limited recrystallization of Fe-bearing samples at relatively high temperatures; dark, isolated spots are single-crystal domains of magnetite.

pendix Table 2[1]). The ordering reflections 101, 015, and 201 (Fig. 2a) have been normalized to the 110 reflection to monitor the evolution of disordering. At 858 K, after 2 min of annealing, this ratio is 0.89 and decreases to 0.58 after 30 min of annealing. No significant further decrease is observed in the following 20 min. At 999 K, the order parameter equilibrates in a few minutes and remains constant at a peak area ratio ~0.21 for almost two hours. Similarly, at 1089 and 1187 K, the normalized peak area ratio I_{201}/I_{110} remained constant with time, confirming the results of Hammouda et al. (2011). We thus decided to collect powder diffractograms after 30 min of annealing at each temperature step for all other samples, to ensure structural equilibrium even at the lowest temperatures. Kinetics is expected to be faster in synthetic samples where crystallite size is in the order of a few micrometers.

Determining ordering for the dolomite-ankerite solid solution

The Rietveld refinement method implemented in the GSAS and EXPGUI programs (Larson and Von Dreele 2000; Toby 2001) was used to analyze the XRPD data, for each temperature and time step. Structural parameters (atomic coordinates, cell parameters, space group) of dolomite, magnesite, aragonite, and magnetite were taken from the ICDD database. For each sample, lattice parameters, scale factor, and two profile parameters of a pseudo-Voigt profile function have been refined and subsequently, all atomic coordinates, U_{iso}, and site occupancies have been refined. U_{iso} have been constrained to be equal in the cation sites, and C-O distances have been constrained to an average 1.3 Å considering high-pressure and temperature data available for carbonates (Ross and Reeder 1992). No constraint has been used for occupancy factors. The results of occupancy refinements are expressed as number of electrons per crystallographic site.

It is worth noting here that at relatively high-Fe contents in dolomite (as in sample S2), random mixing of Fe and Mg in one site leads to a X-ray scattering factor similar to that of Ca in the other site, thus preventing reliable results based on direct site occupancy determinations. To verify if the intensities of superstructure reflections can be used as a proxy for ordering phenomena, we compared the results obtained evaluating ordering by direct site occupancy refinement with superstructure peak intensity ratio (Fig. 3), using, in this latter situation, the square root of the value (Redfern et al. 1989; Dove and Powell 1989; Hammouda et al. 2011). The refined total number of electrons in the two cation site (dotted circles in Fig. 3a) is, within experimental accuracy, equal to the nominal value from chemical composition (dashed line) The order parameter is expressed as $0.5(|elX1–eldis|+|elX2–eldis|)$ normalized to 1, where *el*X1 and *el*X2 stand for the number of electrons in the X1 and X2 sites, and *eldis* is the number of electron per site in the disordered configuration. We compared the evolution of the order parameter derived from structural refinements with evolution of superstructure peaks (201) and (101), normalized to the histogram scale factor. Figure 3 shows that, within experimental accuracy, the information are essentially the same, in agreement also with Parise et al. (2005, their Fig. 5). Parise et al. (2005, p. 82) showed that the results based on the intensity ratios "do give a reasonable estimate of the state of order as complete disorder is approached." This is particularly encouraging as the primary goal of this work is trying to guess the variation of the critical temperature as a function of X_{Fe} and to evaluate the discrepancies of T_c as retrieved by Luth

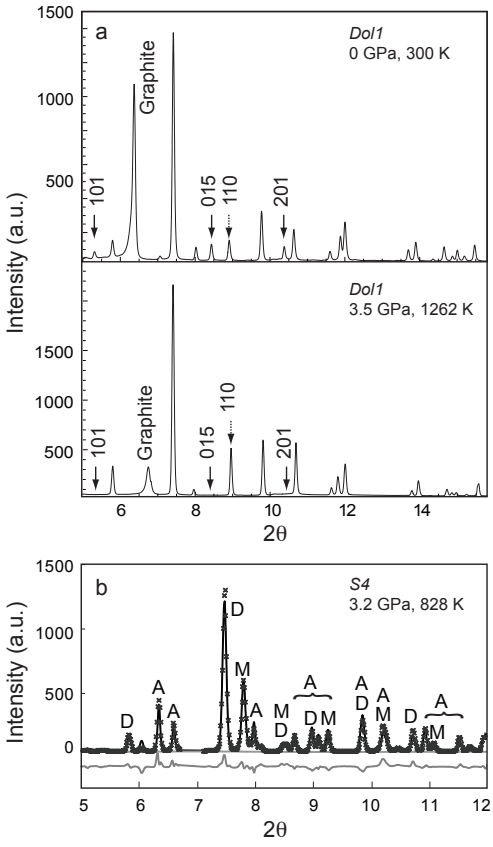

FIGURE 2. (**a**) Synchrotron powder X-ray diffraction for natural dolomite (Dol1) at ambient conditions and at 3.4 GPa and 1262 K. At high temperature the ordering reflections 101, 015, 201 disappear, while the intensity of the reflection 110 does not change with the temperature. (**b**) X-ray powder pattern of sample S4 at 3.2 GPa and 828 K, the phases present are dolomite (D), aragonite (A), and magnesite (M).

(2001), Antao et al. (2004), and Hammouda et al. (2011) on dolomite. As reliable occupancy determinations were obtained for samples S4 and S6 only, we adopt the normalized intensity of I_{101} diffraction peak, which, is not overlapping with any other diffractions (e.g., magnetite) in all the samples considered, to have an internally consistent description of the state of order.

PHASE ASSEMBLAGES FROM IN-SITU EXPERIMENTS

Dolomite-ankerite solid solution

Experimental results are summarized in Table 2. Somewhat unexpected, samples Dol2, S2, and S4 show the nucleation of aragonite+magnesite (Fig. 4), in S2 at temperatures as low as 563 K. The smooth increase of cell parameters, due to the thermal expansion of dolomite (Table 3), across the appearance of aragonite+magnesite supports the assumption that the composition of dolomite during these runs remains constant. In run S2 above 938 K, the abrupt shift observed in dolomite cell parameters may be ascribed to a shift in composition, possibly an incorporation of $CaCO_3$ component.

The nucleation of aragonite+magnesite from dolomite is unexpected at such relatively low-pressure conditions. The results of Luth (2001), Buob et al. (2006), and Shirasaka et al. (2002) would imply an ubiquitous stability of dolomite at pressures lower than ~5 GPa as a result of the bending of the d*P*/

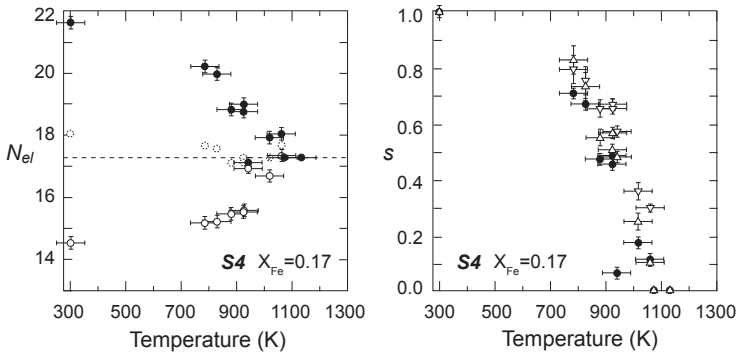

FIGURE 3. (**a**) Experimental site occupancy, expressed as number of electron per cation site (N_{el}; filled circles = X1 site; open circles = X2 site; dotted circles = averaged occupancies, form unconstrained refinement; dashed line = theoretical occupancy for disordered dolomite from stoichiometry). (**b**) Order parameter (triangles pointing upward = square root of normalized 101 peak area; triangles pointing downward = square root of normalized 201 peak area; filled circles = order parameter from refined occupancies).

TABLE 2. Experimental results

	P (GPa)	*T* (K)	Products
Dol1: $Ca_{0.49}Mg_{0.47}Fe_{0.04}CO_3$			
	3.4	300	Dol
	3.4	654	Dol
	3.4	858	Dol
	3.4	999	Dol
	3.4	1089	Dol
	3.4	1187	Dol
	3.4	1262	Dol
Dol2: $Ca_{0.49}Mg_{0.47}Fe_{0.04}CO_3$			
	4.2	300	Dol
	4.2	576	Dol
	4.2	822	Dol+Arag+Mgs
	4.2	960	Dol+Arag+Mgs
	4.2	974	Dol+Arag+Mgs
	4.2	1054	Dol+Arag+Mgs
	4.2	1136	Dol
	4.2	1225	Dol
S2: $Ca_{0.54}Mg_{0.26}Fe_{0.20}CO_3$			
	2.8	327	Dol±Mgt
	2.8	369	Dol±Mgt
	2.8	425	Dol±Mgt
	2.8	504	Arag+Dol±Mgt
	2.8	563	Dol+Arag+Mgs±Mgt
	2.8	621	Dol+Arag+Mgs±Mgt
	2.8	668	Dol+Arag+Mgs±Mgt
	2.8	708	Dol+Arag+Mgs±Mgt
	2.8	757	Dol+Arag+Mgs±Mgt
	2.8	816	Dol+Arag+Mgs±Mgt
	2.8	877	Dol+Arag+Mgs±Mgt
	2.8	938	Dol+Arag+Mgs±Mgt
	2.8	1002	Dol±Mgt
	2.8	1047	Dol±Mgt
	2.8	1110	Dol±Mgt
	2.8	1178	Dol±Mgt
S4: $Ca_{0.52}Mg_{0.40}Fe_{0.08}CO_3$			
	3.2	300	Dol±Mgt
	3.2	785	Dol+Arag+Mgs±Mgt
	3.2	828	Dol+Arag+Mgs±Mgt
	3.2	880	Dol+Arag+Mgs±Mgt
	3.2	924	Dol+Arag+Mgs±Mgt
	3.2	925	Dol±Mgt
	3.2	941	Dol±Mgt
	3.2	1017	Dol±Mgt
	3.2	1061	Dol±Mgt
	3.2	1071	Dol±Mgt
	3.2	1133	Dol±Mgt
S6: $Ca_{0.51}Mg_{0.46}Fe_{0.03}CO_3$			
	2.6	300	Dol±Mgt
	2.6	623	Dol±Mgt
	2.6	673	Dol±Mgt
	2.6	824	Dol±Mgt
	2.6	882	Dol±Mgt
	2.6	957	Dol±Mgt
	2.6	1083	Dol±Mgt
	2.6	1079	Dol±Mgt
	2.6	1140	Dol±Mgt
	2.6	1136	Dol±Mgt
	2.6	1211	Dol±Mgt
S5: $Ca_{0.83}Mg_{0.12}Fe_{0.05}CO_3$			
	3.0	300	Mg-Cc±Mgt
	3.0	459	Mg-Cc±Mgt
	3.0	664	Mg-Cc+Arag+Dol±Mgt
	3.0	745	Mg-Cc+Arag+Dol±Mgt
	3.0	771	Mg-Cc+Arag+Dol±Mgt
	3.0	884	Mg-Cc+Arag+Dol±Mgt
	3.0	913	Mg-Cc+Arag+Dol±Mgt
	3.0	951	Mg-Cc+Arag+Dol±Mgt
	3.0	1002	Mg-Cc+Arag+Dol±Mgt
	3.0	1040	Mg-Cc+Arag+Dol±Mgt
	3.0	1095	Mg-Cc+Arag+Dol±Mgt
	3.0	1149	Mg-Cc+Arag+Dol±Mgt
	3.0	1171	Mg-Cc+Arag+Dol±Mgt
	3.0	1136	Mg-Cc+Arag+Dol±Mgt
	3.0	1235	Mg-Cc+Arag+Dol±Mgt
	3.0	1289	Mg-Cc±Mgt
	3.0	1345	Mg-Cc±Mgt
	3.0	1354	Mg-Cc±Mgt

Notes: The presence of magnetite was detected in all the synthesized samples (refer to the text for the details). Dol = dolomite; Arag = aragonite; Mgs = magnesite; Mg-Cc = Mg-calcite; Mgt = magnetite. In the run *S5* the presence of a disordered carbonate (i.e., called dolomite) was detected observing shoulders on the carbonate peaks of the starting material Mg-calcite (refer to the text for the details).

d*T* slope of the dolomite breakdown reaction at temperatures of ~1200 K (Fig. 4). Nevertheless, the critical experiment of Luth (2001) at 5 GPa, 900 K constraining this bend had pure natural dolomite as starting material but revealed minor amounts of aragonite and magnesite (Table 1 in Luth 2001). This suggests that a driving force enabling aragonite+magnesite nucleation is already present. Similarly, the bend of the d*P*/d*T* slope of the aragonite+magnesite = dolomite reaction in Buob et al. (2006) is constrained by one single experiment at 800 °C, 5.0 GPa with a calcite-magnesite-dolomite starting material.

Hammouda et al. (2011) suggested a much less pronounced decrease of the d*P*/d*T* slope and Morlidge et al. (2006) and Sato

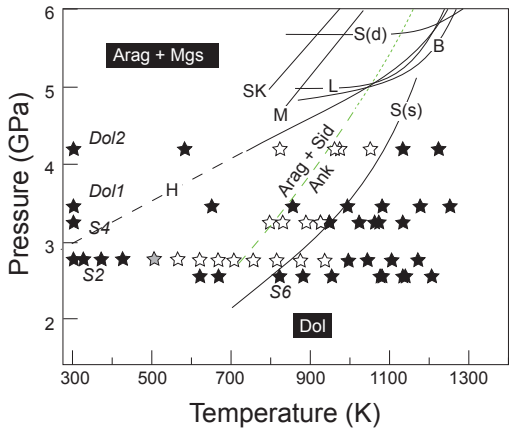

◀**FIGURE 4.** Pressure-temperature trajectories of present experiments in the frame of the breakdown reaction of dolomite into aragonite+magnesite. Our experiments investigated unexplored low pressure-temperature conditions. The reaction boundaries M, L, B, H, and SK refer to the studies of Morlidge et al. (2006), Luth (2001), Buob et al. (2006), Hammouda et al. (2011), and Sato and Katsura (2001), respectively. The curves S(d) and S(s) show the reaction boundaries proposed by Shirasaka et al. (2002) for "synthesis" and "decomposition" experiments. The reaction Arag+Sid = Ank (dashed and dotted gray line) has been constrained by Morlidge et al. (2006). The long dashed lines are low-pressure extrapolation. Open symbols = Dol+Arag +Mgs; filled symbols = Dol; gray symbol = Arag+Dol.

TABLE 3. Cell parameters, normalized peak area ratios (*I*), and site occupancies from Rietveld analysis, at various temperatures and pressures for dolomite-ankerite solid solution

Sample	*P* (GPa)	*T* (K)	*a* (Å)	*c* (Å)	*V* (Å³)	I_{101} norm	I_{201} norm	*Occ* X1 (el)	*Occ* X2 (el)
Dol1	3.4	300	4.773(6)	15.64(2)	308.6(6)	1	1		
	3.4	654	4.772(1)	15.767(3)	310.9(1)	1.00(7)	0.92(7)		
	3.4	858	4.779(1)	15.874(3)	313.9(1)	0.99(5)	0.57(5)		
	3.4	999	4.784(1)	15.945(3)	316.0(1)	0.89(5)	0.21(4)		
	3.4	1089	4.782(1)	16.02(3)	317.2(1)	0.79(4)	0.20(4)		
	3.4	1187	4.779(1)	16.098(3)	318.4(1)	0.031(3)	0.05(1)		
	3.4	1262	4.783(1)	16.158(3)	320.0(1)	0	0		
S2	2.8	327	4.773(5)	15.75(1)	310.8(8)	1	1		
	2.8	369	4.771(5)	15.79(1)	311.4(8)		1		
	2.8	425	4.778(5)	15.79(1)	312.3(2)		0.84(5)		
	2.8	504	4.777(1)	15.810(3)	312.4(2)	0.68(6)	0.61(6)		
	2.8	563	4.777(1)	15.825(3)	312.7(2)	0.80(10)	0.41(10)		
	2.8	621	4.780(1)	15.844(3)	313.5(2)	0.52(11)	0.39(5)		
	2.8	668	4.781(1)	15.858(3)	313.9(2)	0.57(10)	0.33(5)		
	2.8	708	4.782(1)	15.873(3)	314.3(2)	0.43(6)	0.29(6)		
	2.8	757	4.783(1)	15.891(3)	314.8(2)	0.55(6)	0.25(6)		
	2.8	816	4.784(1)	15.925(3)	315.6(2)	0.40(10)	0.33(8)		
	2.8	877	4.787(1)	16.038(3)	318.2(2)	0.29(10)	0.19(5)		
	2.8	938	4.788(1)	16.064(3)	318.9(2)	0.29(10)	0.21(5)		
	2.8	1002	4.789(1)	16.113(3)	320.0(2)	0	0.17(9)		
	2.8	1047	4.789(1)	16.159(3)	320.9(2)	0	0.13(9)		
	2.8	1110	4.791(1)	16.201(3)	322.0(2)	0	0.11(9)		
	2.8	1178	4.792(1)	16.248(3)	323.2(2)	0	0.05(8)		
S4	3.2	300	4.785(8)	15.82(5)	314(2)	1	1	21.6(2)	14.5(2)
	3.2	785	4.780(1)	15.874(3)	314.1(2)	0.69(5)	0.63(5)	20.2(2)	15.2(2)
	3.2	828	4.781(1)	15.912(3)	315.0(2)	0.54(5)	0.57(5)	20.0(2)	15.2(2)
	3.2	880	4.781(1)	15.963(3)	316.0(2)	0.31(3)	0.43(3)	18.8(2)	15.5(2)
	3.2	924	4.782(1)	15.977(3)	316.3(2)	0.26(2)	0.45(2)	18.8(2)	15.5(2)
	3.2	925	4.782(1)	15.994(3)	316.7(2)	0.32(2)	0.43(2)	19.0(2)	15.5(2)
	3.2	941	4.781(1)	16.023(3)	317.1(2)	0.23(2)	0.33(2)	17.1(2)	17.0(2)
	3.2	1017	4.779(1)	16.076(3)	318.0(2)	0.06(3)	0.13(2)	17.9(2)	16.7(2)
	3.2	1061	4.771(1)	16.082(3)	317.0(2)	0.01(1)	0.09(1)	18.1(2)	17.3(2)
	3.2	1071	4.773(1)	16.084(3)	317.3(2)	0	0	17.3	17.3
	3.2	1133	4.773(1)	16.084(3)	317.26(2)	0	0	17.3	17.3
S6	2.6	300	4.778(5)	15.75(1)	311.5(8)	1	1	21.0(1)	12.5(1)
	2.6	623	4.775(5)	15.82(1)	312.5(8)	0.96(6)			
	2.6	673	4.780(5)	15.90(1)	314.5(8)	0.80(6)			
	2.6	824	4.780(1)	15.900(3)	314.7(2)	0.78(5)	0.76(5)	21.0(1)	13.2(1)
	2.6	882	4.782(1)	15.925(3)	315.3(2)	0.75(5)	0.76(5)	20.9(1)	14.2(1)
	2.6	957	4.783(1)	15.952(3)	316.0(2)	0.72(4)	0.77(5)	21.2(1)	14.1(1)
	2.6	1083	4.783(1)	15.987(3)	316.7(2)	0.62(3)	0.71(5)	20.8(1)	14.4(1)
	2.6	1079	4.782(1)	16.035(3)	317.5(2)	0.39(2)	0.62(5)	20.4(1)	14.8(1)
	2.6	1140	4.776(1)	16.076(3)	317.6(2)	0	0	16.5	16.5
	2.6	1136	4.774(1)	16.095(3)	317.7(2)	0	0	16.5	16.5
	2.6	1211	4.771(1)	16.084(3)	317.0(2)	0	0	16.5	16.5

and Katsura (2001) attributed a constant value to the *P*-*T* slope of the aragonite+magnesite = dolomite reaction.

The results of this study support a reaction boundary for a low-Fe dolomite similar to that proposed by Hammouda et al. (2011): if dolomite (e.g., Dol2) is slowly heated at pressures of 4.2 GPa and if the pair aragonite+magnesite is thermodynamically stable at room temperature, we expect nucleation of these carbonates as soon as the kinetic barrier is overstepped, say at $T < 800$ K. Upon further temperature increase run charges would then be in a situation similar to that discussed for the synthesis experiments AM of Shirasaka et al. (2002) where aragonite and magnesite should react to form dolomite. As pointed

out by Shirasaka et al. (2002), the synthesis of dolomite from aragonite+magnesite is kinetically slower then the breakdown reaction of dolomite, and such a metastable synthesis boundary is located at ~1100 K at 4.2 GPa, indeed where aragonite and magnesite disappear in our experiment Dol2.

The assemblage aragonite+magnesite was not observed in experiments Dol1 and S6, performed at 3.4 and 2.6 GPa, respectively. In these experiments, temperature was directly adjusted in the stability field of dolomite, preventing the formation of aragonite+magnesite. In experiment S4 (X_{Fe} = 0.17) the assemblage aragonite+magnesite was observed even though the temperature was directly increased to 785 K. In this bulk composition, the relatively high proportion of Fe is expected to shift the dolomite breakdown reaction toward higher temperatures, broadening the field aragonite+magnesite-siderite solid solution, as suggested by Morlidge et al. (2006). Similarly, this observation applies for the Fe-rich run S2 (X_{Fe} = 0.40).

(Mg,Fe)-calcite

The results of experiment S5 performed on a (Mg,Fe)-calcite of composition $Ca_{0.83}Mg_{0.12}Fe_{0.05}CO_3$ bears on the complexity of the Ca-rich portion of the Ca-Mg-Fe-carbonate ternary, characterized by the occurrence of the univariant reaction dolomite+aragonite = Mg-calcite (Irving and Wyllie 1975; Hermann 2003).

At high-temperature, low-pressure conditions, as employed for synthesis of the starting material used in the experiment S5, calcite forms a continuous solid solution with disordered dolomite. At lower temperatures two- and three-phase fields form as the dolomite-Mg-calcite solvus intersects the aragonite+dolomite/Mg-calcite stability field [Fig. 5; see also Fig. 6a in Irving and Wyllie (1975)]. The topology of phase transformations in this system can be approximated from compositional isobaric-isothermal sections. These were calculated in the system $CaCO_3$-$MgCO_3$-$FeCO_3$ (Fig. 5) employing Perplex 2007 (Connolly 2005), the database of Holland and Powell (1998) for carbonate end-members, and the carbonate solid-solution model of Franzolin et al. (2011). At 3 GPa and relatively low temperature (1073 K in Fig. 5), the ternary diagram is characterized by two mineral assemblages: the two phase field (Mg,Fe)-calcite+aragonite, in the Ca-rich portion of the ternary, and a one-phase field (Mg,Fe)-calcite-dolomite-ankerite solid solution. The bulk composition of experiment S5 (squared symbol in Fig. 5) falls into the two phase field Mg-calcite+aragonite, i.e., the assemblage that persists in the products of experiments S5 up to temperatures in the order of 1200 K.

The boundary delimiting the 1-phase field at 1073 K moves toward the Ca corner with increasing temperature until it intersects the solvus (Mg,Fe)-calcite+dolomite at ~1190 K. The resulting topology of the ternary is then characterized by three 2-phase fields [dolomite+aragonite, (Mg,Fe)-calcite+aragonite, (Mg,Fe)-calcite+dolomite] delimiting the 3-phase field dolomite+aragonite+(Mg,Fe)-calcite. At such conditions, experiment S5 is still in the 2-phase field (Mg,Fe)-calcite+aragonite. At temperatures above the univariant reaction aragonite+dolomite = Mg-calcite (calculated at ~1210 K at 3 GPa), the 3-phase field disappears and the ternary system is characterized by the solvus Mg-calcite+dolomite, the 2-phase field Mg-calcite+aragonite and a broad single-phase field of (Mg,Fe)-calcite-dolomite-ankerite solid solution.

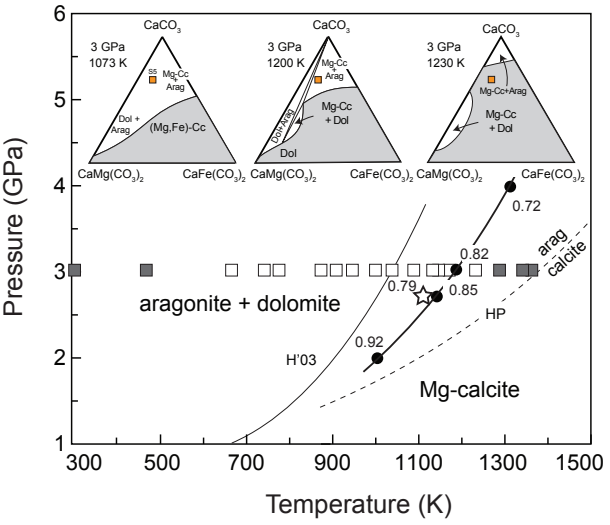

FIGURE 5. *P-T* diagram showing the results of S5 run on (Mg,Fe)-calcite. Filled squares represent the single phase Mg-calcite, empty squares indicate the formation aragonite+dolomite (Table 2). Ternary chemographies, unvariant curves and numbers on filled circles were computed on the basis of the 2002 update of the Holland and Powell database and carbonate solution model by Franzolin et al. (2010). Numbers specify the X_{Ca} content of Mg-calcite along the univariant equilibrium aragonite+dolomite = Mg-calcite in the system $CaCO_3$-$CaMg(CO_3)_2$ (see text). The star stands for the location of the univariant reaction as suggested by Irving and Wyllie (1975) at 2.7 GPa. The location of reaction Mg-calcite = aragonite+dolomite as proposed by Hermann (2003) is reported (H′03).

Calculations predict that the composition S5 should re-equilibrate into the single phase Mg-calcite, but spectra collected at 1235 K yield the persistence of the two coexisting phases Mg-calcite+aragonite. These re-equilibrate to a single phase only at 1289 K. Whether this discrepancy should be ascribed to uncertainties in pressure-temperature determination of the in situ experiments or to imprecisions in the carbonate solution model used remains unclear.

ORDERING IN DOLOMITE SOLID SOLUTION

Disorder in quenched carbonates synthesized ex-situ

To assess the quenchability of disorder/order from ex-situ experiments, we performed synchrotron radiation diffraction on 15 quenched samples (Appendix 1). Appendix Figure 1[1] reports the X-ray diffraction pattern of the sample *r* ($Ca_{0.51}Mg_{0.15}Fe_{0.33}$) CO_3 in which a carbonate of the dolomite-ankerite solid solution coexists with one of the magnesite-siderite solid solution. These syntheses have been performed at 1173 K and 3.5 GPa. The X-ray pattern of sample *r*, as well as patterns of all of the other compositions reported in Appendix 1, does not indicate the presence of superstructure peaks related to $R\bar{3}$ symmetry ("dolomite-like" structure) but the pattern can be fully indexed with supergroup $R\bar{3}c$ ("calcite like"), indicating that at 1173 K the quenched structure is disordered along the dolomite-ankerite join from X_{Fe} = 0.10 to 1.0. Because quenching may promote

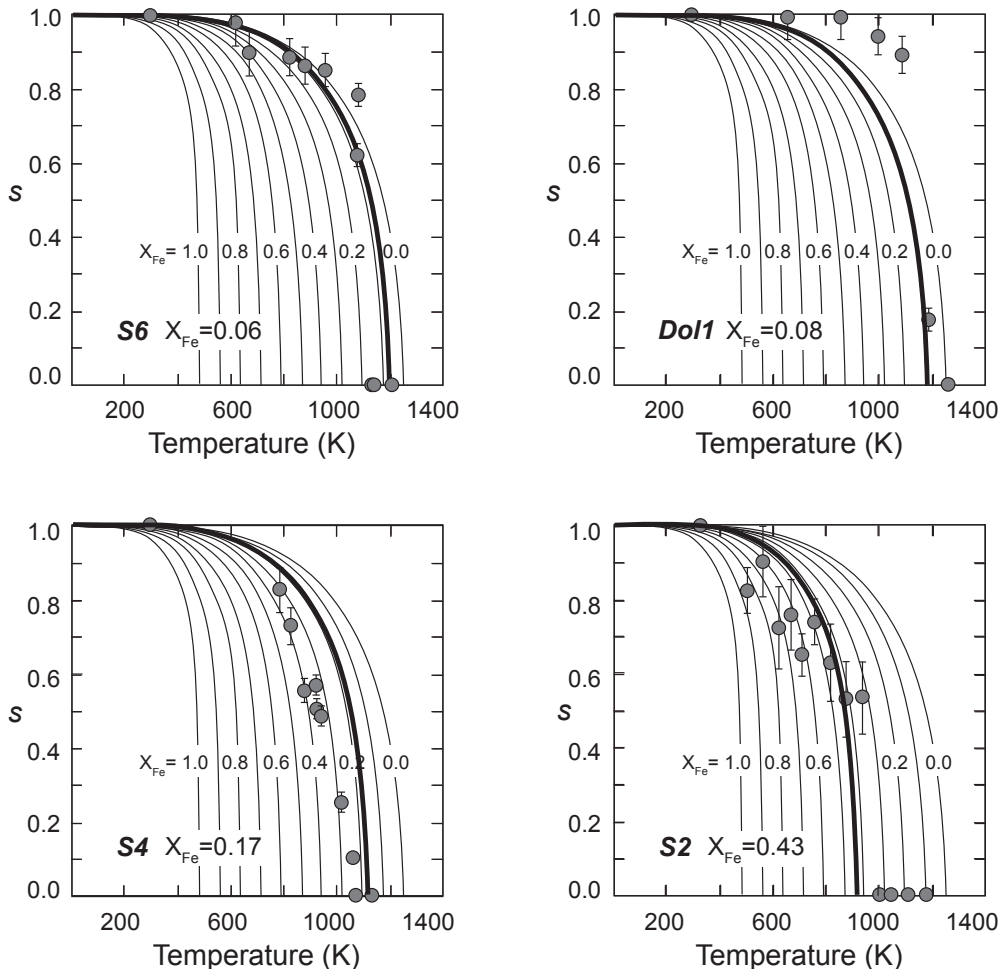

FIGURE 6. Plots of the ordering parameter s, expressed as the normalized peak area ratio I_{101}/I_{110} vs. temperature for the samples S6, Dol1, S4, and S2. The solid lines are the best fit to the experimental data of the model given in Equation 3 (see text). The long-range order parameter (s) calculated for different compositions (X_{Fe}) along the solid solution dolomite-ankerite is given by thin lines.

reordering, the experimental temperature of 1173 K is expected to be in excess of the temperature necessary for complete disordering in Fe-bearing samples, thus, it should represent an upper bound for T_c.

Temperature-composition dependence of the long-range order parameter

In the pure dolomite $CaMg(CO_3)_2$, the long-range order parameter $s = 2X_{Ca}^{M1} - 1$, where X_{Ca}^{M1} is the mole fraction of Ca hosted in the M1 site, describes the partitioning of atomic species (i.e., Ca^{2+} and Mg^{2+}) between two distinct sites. At high temperature these two sites converge and the sites become randomly occupied. This type of order/disorder process has been described with the Bragg-Williams model that, introducing only one energetic parameter related to the critical temperature, formulates the temperature dependence of the order parameter. Antao et al. (2004) proposed a modified Bragg-Williams model taking into account strain interactions resulting from the rotation of the CO_3^{2-} groups and from the size difference between Ca^{2+} and Mg^{2+}. The molar free energy of disordering in dolomite can thus be written as:

$$\overline{G} = \mathrm{R}T_C \left\{ \begin{array}{l} 1 - s^2 + \frac{1}{2}a(s^4 - 1) - \left(\frac{T}{T_C}\right) \\ \left[2\ln 2 - (1+s)\ln(1+s) - (1-s)\ln(1-s)\right] \end{array} \right\} \quad (1)$$

where T_c is the critical temperature, R is the universal gas constant and a, if $\neq 0$, introduces the modification of the Bragg-Williams model. This formulation represents an intermediate case between the Bragg-Williams and the Landau models (Hayward et al. 2000). The Antao-model also better approximates the data on dolomite by Hammouda et al. (2011) when compared to a Landau expansion or to a classic Bragg-Williams model.

To quantify the effect of the solid solution dolomite-ankerite on the disordering mechanism, the compositional term X_{Fe} [Fe/(Fe+Mg)] has to be introduced into the model. Adding Fe-Mg substitution implies coupling between two order parameters (Putnis 1992, p. 266), which further relate to the rotational ordering of the carbonate groups, but the quality of our data do not allow constraining such complex interactions. As a first-order approximation, we therefore treat iron as an "impurity" added

to dolomite, randomly distributed, which can be included in the Landau expansion following Carpenter (1993, Eqs. 33–34). The model proposed by Antao et al. (2004) is therefore modified including the quadratic term $nX_{Fe}(s^2 - 1)$

$$\overline{G} = RT_C \left\{ \begin{array}{l} 1 - s^2 + \frac{1}{2}a(s^4 - 1) + nX_{Fe}(s^2 - 1) - \\ \left(\frac{T}{T_C}\right)\left[2\ln 2 - (1+s)\ln(1+s) - (1-s)\ln(1-s)\right] \end{array} \right\} \quad (2)$$

The equilibrium value of s as a function of temperature and composition is found through the minimum in the function $\overline{G}$ (Eq. 2), i.e., where

$$\frac{\partial \overline{G}(T; s; X_{Fe})}{\partial s} = 0$$

which results in

$$\frac{T}{T_C} = \frac{s(1 - as^2 - nX_{Fe})}{\tanh^{-1} s}. \quad (3)$$

Expression 3 simplifies to the modified Bragg-Williams model (Antao et al. 2004) for a stoichiometric dolomite with $X_{Fe} = 0$.

The normalized peak area ratio I_{101}/I_{110} of the data collected for the samples S2, S4, S6, and Dol1 (Table 3), has been used to fit the model summarized by the Equations 2 and 3. Nonlinear fit leads to a critical temperature T_c = 1243 K (± 63), a = –0.14 (± 0.09), n = –0.61 (± 0.14). Parameter a, introduced by Antao et al. (2004) to account for lattice strain related to rotation of CO_3^{2-} groups, approaches a null value within its confidence interval in our model.

Figure 6 shows the data points and the best fit to the model, evidencing a decrease of the critical temperature with increasing Fe content. In sample S6 (X_{Fe} = 0.06), the ordering reflection I_{101} disappears at ~1140 K, in sample S4 (X_{Fe} = 0.17) the critical temperature approaches ~1000 K, and in sample S2 (X_{Fe} = 0.43) T_c is in the order of 900 K. Our model predict that ordered ankerite should be stable at room temperature, although ordered end-member ankerite has neither been found nor synthesized (see also Morlidge et al. 2006). However, the very low-temperatures predicted for ordering might inhibit the ordering process.

Even though this is the first study that explores the Fe influence for the cation disorder in dolomite, the disordering process for stoichiometric dolomite has been already investigated by Luth (2001), via quench techniques, and in situ by Antao et al. (2004) and by Hammouda et al. (2011). Antao et al. (2004) determined the structure of a nearly stoichiometric dolomite at 3 GPa with in situ synchrotron X-ray diffraction similar to our study; the results should therefore be comparable. Antao et al. (2004) described the order/disorder transition with a modified Bragg-Williams model (Eq. 1) locating the critical temperature at 1466 K. Our model (Eq. 2) applied to pure Ca-Mg-dolomite locates the critical temperature at 1243 K, a disorder temperature significantly lower than that of Antao et al. (2004). An overestimation of the experimental temperatures of Antao et al. (2004) was also suggested by Hammouda et al. (2011) who employed a multi-anvil apparatus and synchrotron radiation in energy dispersive mode locating the disordering temperature at ~1340 K at 3.4– 4 GPa. Our structure refinements performed ex-situ on quenched Fe-dolomites in the range X_{Fe} = 0.10 to 1.0 resulted in complete disordering at T = 1173 K for all samples. This further corroborates the conclusion that dolomite disordering should occur for dolomite at ~1200 K, as observed in in situ experiments. A possible contribution to discrepancies between the experimental studies comes from the redox state of the experimental charges at run conditions. Dolomite may accommodate Fe^{3+} compensated by incorporation of B or by the creation of cation vacancy for each pair of Fe^{3+} impurities (Papathanassiou 2003). Antao et al. (2004) performed experiments on samples contained in Au capsules, at unbuffered oxygen conditions, although Fe-contents in Eugui dolomite is very low. Hammouda et al. (2011) had Pt powder in contact with the charge, an assemblage that has the oxidizing equilibrium Pt-PtO_2 as an upper bound and no lower bound. In experiments presented here, Fe-bearing dolomite samples are in contact with graphite. As a consequence oxygen fugacity has the equilibrium CCO as an upper bound and the equilibrium dolomite = graphite+periclase+aragonite as a lower bound, ~3 log units below CCO. At such conditions we might expect low Fe^{3+} in carbonates synthesized. However, whether the diffusion of boron, commonly used in all in situ experiments (as boron epoxy or boron nitride) may affect Fe-oxidation state is entirely unexplored.

Concluding remarks

The temperature and composition dependence of the degree of order in dolomite is crucial to understand the thermodynamics and phase relations of carbonates in the $CaCO_3$-$MgCO_3$-$FeCO_3$ ternary. Carbonates in this system are fundamental for the comprehension and prediction of the fate of subducted carbon in the mantle, where carbon recycling is governed by Fe-bearing mineral phases hosted in the oceanic lithosphere. Our direct observations of the order/disorder state in intermediate compounds (i.e., dolomite/ankerite) thus allow improving solid-solution models for ternary carbonates, the ultimate goal being to reliably predict phase relations involving ternary carbonates.

Acknowledgments

The constructive reviews by two anonimous reviewers significantly improved the manuscript. We are thankful to S. Tumiati for discussions improving the manuscript and for help performing synchrotron experiments (exp. n. HS3709). Thanks to J.P. Perillat and M. Mezouar for technical support at the beamline ID27-ESRF and Michael Hanfland for data collection on ID09 beamline.

This work was funded by the European Commission through the Marie Curie Research training Network "c2c," Contract No. MRTN-CT-2006-035957 and by Italian MIUR PRIN 2009XRH8JJ.

References cited

Antao, S.M., Mulder, W.H., Hassan, I., Crichton, W.A., and Parise, J.B. (2004) Cation disorder in dolomite, $CaMg(CO_3)_2$, and its influence on the aragonite plus magnesite ↔ dolomite reaction boundary. American Mineralogist, 89, 1142–1147.

Besson, J.M., Nelmes, R.J., Hamel, G., Loveday, J.S., Weill, G., and Hull, S. (1992) Neutron powder diffraction above 10 GPa. Physica B, 180, 907–910.

Buob, A., Luth, R.W., Schmidt, M.W., and Ulmer, P. (2006) Experiments on $CaCO_3$-$MgCO_3$ solid solutions at high pressure and temperature. American Mineralogist, 91, 435–440.

Carpenter, M.A. (1993) Thermodynamics of phase transitions in minerals: A macroscopic approach. In G.D. Price and N.L. Ross, Ed., The Stability of Minerals. The Mineralogical Society Series, 3, p. 172–215. Springer, Berlin.

Connolly, J.A.D. (2005) Computation of phase equilibria by linear programming: A tool for geodynamic modeling and its application to subduction zone decar-

bonation. Earth and Planetary Science Letters, 236, 524–541.
Crichton, W.C. and Mezouar, M. (2002) Noninvasive pressure and temperature estimation in large-volume apparatus by equation-of-state cross-calibration. High Temperatures–High Pressures, 34, 235–242.
Dasgupta, R. and Hirschmann, M.M. (2006) Melting in the Earth's deep upper mantle caused by carbon dioxide. Nature, 440, 659–662.
Dasgupta, R., Hirschmann, M.M., and Withers, A.C. (2004) Deep global cycling of carbon constrained by the solidus of anhydrous, carbonated eclogite under upper mantle conditions. Earth and Planetary Science Letters, 227, 73–85.
Dasgupta, R., Hirschmann, M.M., and Dellas, N. (2005) The effect of bulk composition on the solidus of carbonated eclogite from partial melting experiments at 3 GPa. Contributions to Mineralogy and Petrology, 149, 288–305.
Dove, M.T. and Powell, B.M. (1989) Neutron diffraction study of the tricritical orientational order/disorder phase transition in calcite at 1260 K. Physics and Chemistry of Minerals, 16, 503–507.
Falloon, T.J. and Green, D.H. (1989) The solidus of carbonated, fertileperidotite. Earth and Planetary Science Letters, 94, 364–370.
Franzolin, E., Schmidt, M.W., and Poli, S. (2011) Ternary Ca-Fe-Mg-carbonates: subsolidus phase relations at 3.5 GPa and a thermodynamic solid solution model including order/disorder. Contributions to Mineralogy and Petrology, 161, 213–227.
French, B.M. (1971) Stability relations of siderite ($FeCO_3$) in system Fe-C-O. American Journal of Science, 271, 37–78.
Gieré, R. (1990) Quantification of element mobility at a tonalite/dolomite contact, 158 p. Ph.D. dissertation, ETH, Zurich.
Goldsmith, J.R., Graf, D.L., Witters, J., and Northrop, D.A. (1962) Studies in the System $CaCO_3$-$MgCO_3$-$FeCO_3$. 1. Phase Relations. 2. A Method for Major-Element Spectrochemical Analysis. 3. Compositions of Some Ferroan Dolomites. Journal of Geology, 70, 659–688.
Grassi, D. and Schmidt, M.W. (2011) The melting of carbonated pelites from 70 to 700 km depth. Journal of Petrology, 52, 765–789.
Hammersley, A.P., Svensson, S.O., Hanfland, M., Fitch, A.N., and Häusermann, D. (1996) Two-dimensional detector software: From real detector to idealized image or two-theta scan. High Pressure Research, 14, 235–245.
Hammouda, T. (2003) High-pressure melting of carbonated eclogite and experimental constraints on carbon recycling and storage in the mantle. Earth and Planetary Science Letters, 214, 357–368.
Hammouda, T., Andrault, D., Koga, K., Katsura, T., and Martin, A.M. (2011) Ordering in double carbonates and implications for processes at subduction zones. Contributions to Mineralogy and Petrology, 161, 439–450.
Hayward, S.A., del Cerro, J., and Salje, E.K.H. (2000) Antiferroelectric phase transition in titanite: excess entropy and short range order. American Mineralogist, 85, 557–562.
Hermann, J. (2003) Carbon recycled into deep Earth: Evidence from dolomite dissociation in subduction-zone rocks: Comment and Reply. Geology, 31, e4–e5.
Holland, T.J.B. and Powell, R. (1998) An internally consistent thermodynamic data set for phases of petrological interest. Journal of Metamorphic Geology, 16, 309–343.
Irving, A. and Wyllie, P. (1975) Subsolidus and melting relationships for calcite, magnesite and the join $CaCO_3$–$MgCO_3$ to 36 kb. Geochimica et Cosmochimica Acta, 39, 35–53.
Larson, A.C. and Von Dreele, R.B. (2000) General structure analysis system (GSAS). Los Alamos National Laboratory Report, LAUR 86-748.
Luth, R.W. (2001) Experimental determination of the reaction aragonite plus magnesite = dolomite at 5 to 9 GPa. Contributions to Mineralogy and Petrology, 141, 222–232.
Markgraf, S.A. and Reeder, R.J. (1985) High-temperature structure refinements of calcite and magnesite. American Mineralogist, 70, 590–600.
Martinez, I., Zhang, J.Z., and Reeder, R.J. (1996) In situ X-ray diffraction of aragonite and dolomite at high pressure and high temperature: Evidence for dolomite breakdown to aragonite and magnesite. American Mineralogist, 81, 611–624.
Mezouar, M., Le Bihan, T., Libotte, H., Le Godec, Y., and Hausermann, D. (1999) Paris-Edinburgh large-volume cell coupled with a fast imaging-plate system for structural investigation at high pressure and high temperature. Journal of Synchrotron Radiation, 6, 1115–1119.
Molina, J.F. and Poli, S. (2000) Carbonate stability and fluid composition in subducted oceanic crust: an experimental study on H_2O-CO_2-bearing basalts. Earth and Planetary Science Letters, 176, 295–310.
Morlidge, M., Pawley, A., and Droop, G. (2006) Double carbonate breakdown reactions at high pressures: an experimental study in the system CaO-MgO-FeO-MnO-CO_2. Contributions to Mineralogy and Petrology, 152, 365–373.
Papathanassiou, A.N. (2003) Study of the polarizable centers in single-crystal dolomite [$CaMg(CO_3)_2$] rich in Fe^{3+} impurities by thermally stimulated depolarization current spectroscopy. Journal of Physics and Chemistry of Solids, 64, 171–175.
Parise, J.B., Antao, S.M., Martin, C.D., and Crichton, W. (2005) Diffraction studies of order-disorder at high pressures and temperatures. Powder Diffraction, 20, 80–86.
Philipp, R.W. (1998) Phasenbeziehungen im System MgO-H_2O-CO_2-NaCl, 185p. PhD Dissertation, ETH, Zurich.
Poli, S., Franzolin, E., Fumagalli, P., and Crottini, A. (2009) The transport of carbon and hydrogen in subducted oceanic crust: An experimental study to 5 GPa. Earth and Planetary Science Letters, 278, 350–360.
Putnis, A. (1992) Introduction to Mineral Sciences. Cambridge University Press, U.K.
Redfern, S.A.T., Salje, E., and Navrotsky, A. (1989) High-temperature enthalpy at the orientational order-disorder transition in calcite: implications for the calcite/aragonite phase equilibrium. Contributions to Mineralogy and Petrology, 101, 479–484.
Rosenberg, P.E. (1967) Subsolidus relations in system $CaCO_3$-$MgCO_3$-$FeCO_3$ between 350 and 550 °C. American Mineralogist, 52, 787–796.
Ross, N.L. and Reeder, R.J. (1992). High pressure structural study of dolomite and ankerite. American Mineralogist, 77, 412–421.
Sato, K. and Katsura, T. (2001) Experimental investigation on dolomite dissociation into aragonite plus magnesite up to 8.5 GPa. Earth and Planetary Science Letters, 184, 529–534.
Shirasaka, M., Takahashi, E., Nishihara, Y., Matsukage, K., and Kikegawa, T. (2002) In situ X-ray observation of the reaction dolomite = aragonite plus magnesite at 900–1300 K. American Mineralogist, 87, 922–930.
Toby, B.R. (2001) EXPGUI, a graphical user interface for GSAS. Journal of Applied Crystallography, 34, 210–221.
Tumiati, S., Fumagalli, P., and Poli, S. (2012) An experimental study on COH-bearing peridotite up to 3.2 GPa and implications for crust-mantle recycling. Journal of Petrology, in press.
Wallace, M.E. and Green, D.H. (1988) An experimental determination of primary carbonatite magma composition. Nature, 335, 343–346.
Wu, T.C., Shen, A.H., Weathers, M.S., Bassett, W.A. (1995) Anysotropic thermal expansion of calcite at high pressures: an in-situ X-ray diffraction study in a hydrothermal diamond anvil cell. American Mineralogist, 80, 941–946.
Yaxley, G.M. and Brey, G.P. (2004) Phase relations of carbonate-bearing eclogite assemblages from 2.5 to 5.5 GPa: Implications for petrogenesis of carbonatites. Contributions to Mineralogy and Petrology, 146, 606–619.

Manuscript received February 6, 2012
Manuscript accepted June 25, 2012
Manuscript handled by Simon Redfern